

Correlation between primary phases and atomic clusters in a Zr-based metallic glass

X. J. Liu, G. L. Chen, and C. T. Liu

Citation: *J. Appl. Phys.* **108**, 123516 (2010); doi: 10.1063/1.3525985

View online: <http://dx.doi.org/10.1063/1.3525985>

View Table of Contents: <http://jap.aip.org/resource/1/JAPIAU/v108/i12>

Published by the [American Institute of Physics](#).

Related Articles

Electrical and spectroscopic analysis in nanostructured SnO₂: “Long-term” resistance drift is due to in-diffusion
J. Appl. Phys. **110**, 093711 (2011)

Study on the structural and physical properties of ZnO nanowire arrays grown via electrochemical and hydrothermal depositions
J. Appl. Phys. **110**, 094310 (2011)

Silver/silicon dioxide/silver sandwich films in the blue-to-red spectral regime with negative-real refractive index
Appl. Phys. Lett. **99**, 181117 (2011)

Fluorescence enhancement of light-harvesting complex 2 from purple bacteria coupled to spherical gold nanoparticles
Appl. Phys. Lett. **99**, 173701 (2011)

Optical study of the effect of the impurity content on the ferroelectric properties of Er³⁺ doped SBN glass-ceramic samples
J. Appl. Phys. **110**, 084113 (2011)

Additional information on *J. Appl. Phys.*

Journal Homepage: <http://jap.aip.org/>

Journal Information: http://jap.aip.org/about/about_the_journal

Top downloads: http://jap.aip.org/features/most_downloaded

Information for Authors: <http://jap.aip.org/authors>

ADVERTISEMENT

**AIP**Advances

Submit Now

**Explore AIP's new
open-access journal**

- **Article-level metrics
now available**
- **Join the conversation!
Rate & comment on articles**

Correlation between primary phases and atomic clusters in a Zr-based metallic glass

X. J. Liu,^{1,2,a)} G. L. Chen,¹ and C. T. Liu^{2,a)}

¹State Key Laboratory for Advanced Metals and Materials, University of Science and Technology Beijing, Beijing 100083, People's Republic of China

²Department of Mechanical Engineering, The Hong Kong Polytechnic University, Hung Hom, Kowloon, Hong Kong, People's Republic of China

(Received 6 August 2010; accepted 12 November 2010; published online 23 December 2010)

Atomic clusters existing in the $Zr_{65}Ti_{10}Ni_{25}$ metallic glass and primary phases generated during crystallization were studied by x-ray scattering and high-resolution transmission microscopy. An intrinsic correlation between the atomic clusters and the primary phases has been revealed. It is found that there are topological icosahedral short-range orders (ISROs) in the as-cast sample in addition to fcc- Zr_2Ni -type chemical SROs. These topological ISRO and fcc- Zr_2Ni -type chemical SRO can simultaneously quasicrystallize/crystallize into the corresponding nanoscaled icosahedral quasicrystalline phase (I-phase) and fcc- Zr_2Ni crystal as primary products during crystallization. The synchronic precipitation of these two metastable phases can be understood in terms of their structural similarity between the fcc- Zr_2Ni and I-phase in local atomic configuration. In comparison with fcc- Zr_2Ni crystal, the I-phase has a smaller size and lower volume fraction due to its lower growth rate attributed to its more complex composition and higher structural symmetry. The competitive growth between these two phases results in the development of nanostructured materials in this alloy after annealing. © 2010 American Institute of Physics.

[doi:10.1063/1.3525985]

I. INTRODUCTION

Since the first metallic glass (MG) was synthesized through rapid quenching of liquid in the early 1960 s,¹ tremendous efforts have been devoted to the fundamental researches of atomic structures and its relationship to glass forming ability, thermal stability, and crystallization behavior of MGs.^{2–8} So far, it is widely accepted that there are various short-range orders (SROs) and medium-range orders (MROs) in supercooled liquids and MGs,^{3,9–12} and these atomic clusters are strongly related to glass formation and devitrification behaviors.^{8,13,14} In particular, the icosahedral SRO (ISRO) has been considered as the basic building block of supercooled liquids and MGs.^{3,15–17} Due to its incompatibility to crystal symmetry, it was also suggested to be responsible for the glass formation and thermal stability of MGs by stabilizing the supercooled liquids. Meanwhile, both experimental and theoretical studies indicated that the ISRO has a significant influence on the crystallization behavior of MGs.^{7,8,15} For instance, Kelton *et al.*¹⁸ revealed that the degree of ISRO increases with decreasing temperature in the $Zr_{39.5}Ti_{39.5}Ni_{21}$ melt until the icosahedral quasicrystalline phase (I-phase) precipitates. This finding confirmed the Frank's hypothesis that the local structures in undercooled liquid contain a significant degree of ISRO,¹⁹ they create a nucleation barrier to form crystallographic phases and then making the large undercooling available in metallic liquid. As such, the I-phase has smaller nucleation barrier as compared with crystal phases and preferentially becomes the primary phase during crystallization of MGs.^{20–22}

On the other hand, in addition to topological ISRO, the atomic clusters with the characteristic of lattice-type chemical SROs (CSROs) due to the effect of chemical interactions among unlike constituent elements are also observed in many multicomponent MGs.^{10,11,17,23} These lattice-type SROs and MROs can act as prenuclei or nucleation sites during crystallization of MGs. As an example, the fcc- Zr_2Ni SRO and MRO which were often observed in Zr-based MGs and their undercooled liquids can directly transform into the crystalline counterpart, the fcc- Zr_2Ni crystal, when the MGs were annealed.^{24,25} Despite the correlation between the primary phases and the atomic clusters in MGs has been perceived, a direct experimental evidence that bridges the link between the primary phases and the ISRO and CSRO in MGs is still missing. Furthermore, the competitive growth between ISRO and CSRO during crystallization has not been studied.

In this study, we selected a $Zr_{65}Ni_{25}Ti_{10}$ MG as the model material, which was expected to possess comparable ISRO and CSRO in the as-cast sample and was designed based on the following considerations: (1) its composition is close to Zr_2Ni phase, in which the Zr_2Ni -like CSRO or MRO is expected to develop and (2) titanium is an favorable element for forming ISRO in Zr-based MGs.^{8,26} Actually, I-phase was often reported in the Zr–Ti–Ni alloy system, especially the stable I-phase phase was found at the vicinity of $Zr_{41.5}Ti_{41.5}Ni_{17}$.²⁷ As we expected, the structural analyses indicate there coexist fcc- Zr_2Ni -type SRO and ISRO in the $Zr_{65}Ni_{25}Ti_{10}$ MG. The crystallization investigation suggests that both the nanoscaled fcc- Zr_2Ni and I-phase can be precipitated as the primary phases simultaneously when the sample was annealed in its supercooled liquid region, indi-

^{a)}Electronic addresses: xjliu@ustb.edu.cn and ct.liu@inet.polyu.edu.hk.

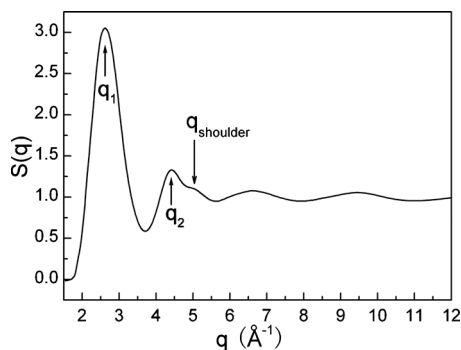


FIG. 1. Structural factor of the as-cast $Zr_{65}Ti_{10}Ni_{25}$ MG. The appearance of shoulder on the second peak indicates the existence of ISRO in the as-cast sample.

cating the good possibility to form nanocrystals in this alloy, and providing a new scenario for understanding the crystallization behavior of MGs.

II. EXPERIMENTAL PROCEDURE

The master alloy with a nominal composition of $Zr_{65}Ti_{10}Ni_{25}$ (at. %) was prepared by arc melting under a Ti-gettered pure argon atmosphere, using pure metals [$\geq 99.9\%$ (wt %)] as charge materials. Then, the amorphous ribbons were produced by a single roller melt-spinning technique under argon atmosphere. X-ray scattering experiment was performed on the SIEMENS D5000 diffractometer with Mo $K\alpha$ radiation ($\lambda = 0.7093 \text{ \AA}$). The diffraction data were collected at ambient temperature in flat transmission geometry and the scattering angle 2θ covered the range from 4° to 120° . The characteristic temperatures were determined with NETZSCH STA 449C differential scanning calorimeter (DSC) at a heating rate of 20 K/min. To study its primary crystallization behavior, the as-cast sample was annealed in its supercooled liquid region (615 K) under a vacuum of 4.0×10^{-3} Pa. Thin foil samples for high-resolution transmission electron microscopy (HRTEM) analysis were first prepared by twin-jet electrolytic polishing in a mixing solution of 90 vol % methanol and 10 vol % perchloric acid under 240 K. The electropolished and perforated samples were then cleaned by a brief (0.5 h) ion milling process to remove some residual surface contamination. The HRTEM observations were performed at Tecnai G2 F20 S-Twin field emission gun microscope embedded Oxford energy dispersive x-ray (EDX) spectroscopy, operated at 200 kV. The images were collected on a charge-coupled device camera and image analysis was carried out using the software DIGITALMICROGRAPH 3.5.2 of Gatan Inc.

III. RESULTS AND DISCUSSION

Figure 1 shows the structural factor extracted from the x-ray scattering data for the as-cast $Zr_{65}Ti_{10}Ni_{25}$ MG. The raw data were corrected for air scattering, polarization and absorption, and inelastic scattering by using the program PDFGETX2.²⁸ The total structure factor $S(q)$ was determined in terms of the definition of Faber and Ziman.²⁹ As observed in many Zr–Ti–Ni alloys and other glassy alloys bearing local icosahedral orders,^{7,18,30} a shoulder on the high- q side of

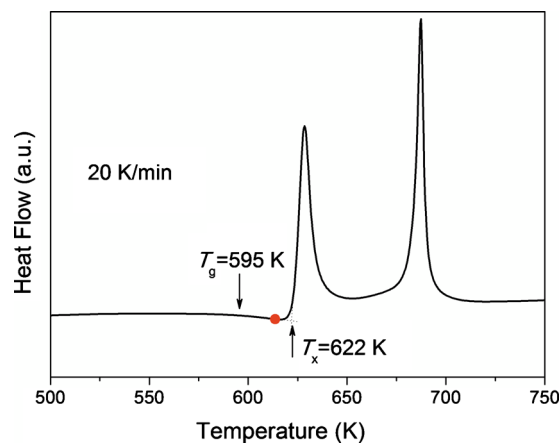


FIG. 2. (Color online) DSC curve of the as-cast $Zr_{65}Ti_{10}Ni_{25}$ MG at a heating rate of 20 K/min. The red point denotes the annealing temperature 615 K.

the second peak in $S(q)$ is also clearly found in the present case. The relative position of the first two peaks in $S(q)$, $q_2/q_1 = 1.70$, and the ratio of the shoulder peak to the first one, $q_{\text{shoulder}}/q_1 = 1.94$, are in good agreement with those theoretical values for a glass with perfect ISRO,³¹ $q_2/q_1 = 1.71$ and $q_{\text{shoulder}}/q_1 = 2.04$. This firmly confirms the presence of ISRO in the as-cast sample although the ISRO here is little distorted with respect to the perfect ISRO. Meanwhile, the fcc- Zr_2Ni -like MRO with a size of 1–2 nm has been identified through HRTEM coupled with nanobeam electron diffraction techniques in this alloy.^{23,24} Based on these results, we can safely conclude that there coexist topological ISRO and chemical lattice-type SRO and MRO in the as-cast $Zr_{65}Ti_{10}Ni_{25}$ MG.

Figure 2 is the DSC curve of the as-cast sample at the heating rate of 20 K/min. According to the endothermic and exothermic events appeared in Fig. 2, the glass transition temperature T_g and the onset of crystallization temperature T_x are estimated to be 595 K and 622 K, respectively. There are two separate exothermic peaks caused by crystallization events, indicating the crystallization is proceeded by a two-step model. To explore what primary phase precipitates during crystallization, the sample was isothermally annealed at 615 K for different durations. The primary phases identified by x-ray diffraction (XRD) results are mainly metastable fcc- Zr_2Ni compounds [space group $Fd\bar{3}m$ (227), $a = 12.27 \text{ \AA}$],²⁴ the average size of which was determined to be about 26 nm as estimated from the x-ray line broadening according to the Scherrer formula.³² Figure 3 shows the TEM bright-field image of the sample annealed at 615 K for 15 min. From the image, it is found that the precipitates can be mainly divided into two kinds according to their sizes and amounts: one is of large size and amount (marked by green circles) and the other is of small size and amount (marked by red circles). Figure 4 displays the typical HRTEM image of the large particles (marked by green circles in Fig. 3) precipitated from the amorphous matrix in the sample after annealing. The inset at the up left corner in Fig. 4 is the inverse Fourier transformation (IFT) image of selected area (enclosed by the red square), which clearly shows the lattice fringe. The interplanar spacing was measured to be 0.25 nm,

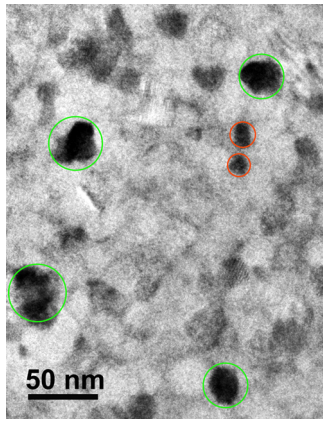


FIG. 3. (Color online) TEM bright-field image of the sample annealed at 615 K for 15 min. The green and red circles mark two kinds of precipitates, respectively.

which corresponds the value of crystal plane (422) in the fcc-Zr₂Ni phase. This result is consistent with previous XRD analysis. In our previous work,^{24,25} the atomistic mechanism of precipitating the fcc-Zr₂Ni nanocrystal from Zr-based MGs has been revealed. It was found that, under a large undercooling condition, the fcc-Zr₂Ni-like MRO pre-existing in MGs can directly grow up into fcc-Zr₂Ni nanocrystals, which was well explained in terms of nonclassical nucleation theory.³³

As mentioned above, the fcc-Zr₂Ni SRO/MRO in MGs can crystallize into crystalline counterparts during annealing. Then, the question whether the ISRO is also able to quasicrystallize into I-phase is raised naturally. In view of the fact that the ISRO directly quasicrystallized into I-phase as the primary phase during solidification of Zr_{39.5}Ti_{39.5}Ni₂₁ melts and I-phase was observed frequently during primary crystallization of Zr-based MGs,^{18,21,22} it is supposed that I-phase should be involved in the primary phases during crystallization of the Zr₆₅Ti₁₀Ni₂₅ MG. In order to confirm this assumption, a careful survey based on HRTEM experiments was conducted. As indicated by the above results, the large particles observed in the bright-field TEM image (Fig. 3) are fcc-Zr₂Ni phases. Thus, here we focus on the small ones. Figure 5(a) shows the typical HRTEM image of the tiny particles (marked by red circles in Fig. 3) formed in the

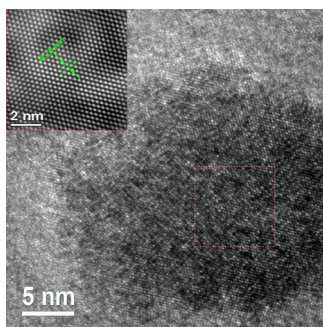


FIG. 4. (Color online) HRTEM image of an fcc-Zr₂Ni phase (the large particles marked by green circles in Fig. 3) precipitated from the sample annealed at 615 K for 15 min. The inset shows the IFT image of the selected area (enclosed by the red square). The measurement of its interplanar spacing identifies the nanoparticle as the fcc-Zr₂Ni structure.

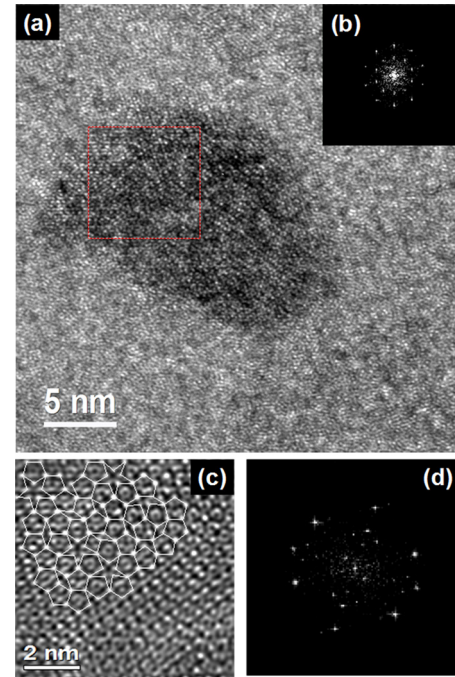


FIG. 5. (Color online) (a) HRTEM image of an I-phase (the small particles marked by red circles in Fig. 3) precipitated from the sample annealed at 615 K for 15 min. (b) FT pattern of the selected area in (a), showing the fivefold symmetry. (c) IFT image of the selected area (enclosed by the red square) in (a), the white line plot is the result of linking the bright points and shows the fivefold symmetries of arrangement of the atomic units in the high symmetrical I-phase. (d) FT pattern of the I-phase, showing twofold zone axes.

Zr₆₅Ti₁₀Ni₂₅ MG after annealing at 615 K for 15 min. Figures 5(b) and 5(d) are Fourier transformation (FT) patterns of HRTEM images, displaying the fivefold and twofold symmetries in the I-phase, respectively. Figure 5(c) is the IFT image of the selected area (enclosed by the red square) in Fig. 5(a), showing the tenfold and fivefold symmetries of arrangement of the atomic units in the high symmetrical I-phase. These results indicate that the small particles shown in Fig. 3 are corresponding to the I-phase. By carefully scrutinizing several HRTEM images of the I-phase particles and the TEM bright-field image (Fig. 3), it is found that, compared with the fcc-Zr₂Ni nanocrystal (~26 nm), the I-phase has a smaller size (~10 nm) in addition to amount. Due to the limitation of particle size, a quantitative determination of the composition of I-phase is not easy for the EDX method. However, the qualitatively EDX analysis (not shown here) indicates that the I-phase is a Zr-rich phase including Zr, Ni, and Ti constituents, implying that it is metastable due to the fact that the stable I-phase has a composition of Zr_{41.5}Ti_{41.5}Ni₁₇ in this system.²⁷ This observation gives a solid evidence to ascertain the formation of I-phase during the primary crystallization although its volume fraction is not appreciable enough to be detected by XRD measurement. So far, it is sure that the ISRO in the as-cast sample can also quasicrystallize into the corresponding I-phase as a primary phase during crystallization of the Zr₆₅Ti₁₀Ni₂₅ MG.

The present case poses a new scenario of primary crystallization that two metastable phases precipitate out simultaneously during annealing, while this phenomenon is rarely

reported in the literature. In previous reports,^{21,22,34,35} the primary phase includes only one metastable phase, either an fcc crystalline phase or an I-phase, precipitated from amorphous matrix. Eckert *et al.*²⁰ found that the metastable I-phase and fcc-Zr₂Ni-type phase can be formed simultaneously as primary phases during crystallization of Zr₆₅Al_{7.5}Cu_{17.5}Ni₁₀ MG when the alloy contains a certain amount of oxygen, indicating that the primary phase is sensitive to oxygen content of the materials. For the present case, the starting materials are of high purity and the vacuum was strictly controlled during the preparation and annealing process. Therefore, we believe that the oxygen effect is not the governing factor in this case, and the synchronic precipitation of two metastable fcc-Zr₂Ni and I-phase should be mainly attributed to their structural similarity. Although they have incompatible crystallographic symmetry globally, there are also icosahedral atomic clusters in local atomic configurations of the fcc-Zr₂Ni crystal structure.^{34,35} Indeed, the fcc-Zr₂Ni was often believed to be a crystalline approximant of the Zr-based I-phase due to their structural similarity,³⁵ suggesting that they have no significant difference in nucleation barrier. As such, they have almost the same priority to precipitate during annealing from the thermodynamic point of view. Then, it is not surprised that the fcc-Zr₂Ni SRO and ISRO in the Zr₆₅Ti₁₀Ni₂₅ MG can crystallize/quasicrystallize into corresponding metastable crystals and quasicrystals during primary crystallization. The EDX analysis indicates that the specific composition of I-phase can be roughly identified as Zr_{56.5}Ni_{29.1}Ti_{14.4}, implying that the growth of I-phase needs a significant rearrangement of Zr and Ti atoms while only the Ti atoms have to be expelled in the growth of fcc-Zr₂Ni phase. Due to this kinetic consideration as well as its higher structural symmetry than the fcc-Zr₂Ni crystal, the I-phase may grow slower, leading to its smaller size and lower volume fraction. In addition, this phase competition and impingement during the formation of these two phases could make the phase growth sluggish and then provides a possibility to produce nanostructured materials through crystallization. In fact, the nanograined structures with an average size of about 17 nm have been confirmed by the *in situ* small angle x-ray scattering data when the alloy was annealed at 615 K for 40 min.³⁶

IV. CONCLUSION

There are topological ISROs in the as-cast Zr₆₅Ti₁₀Ni₂₅ MG in addition to fcc-Zr₂Ni-type CSROs/MROs. When the alloy was annealed in its supercooled liquid region (615 K) for 15 min, these topological ISRO and chemical fcc-Zr₂Ni-type SRO can simultaneously quasicrystallize/crystallize into the corresponding nanoscaled I-phase and fcc-Zr₂Ni crystal as primary products during crystallization. This results can be explained in terms of their structural similarity between the fcc-Zr₂Ni and I-phase in local atomic configuration. Meanwhile, in comparison with fcc-Zr₂Ni crystal, the I-phase has a smaller size and lower volume fraction due to its lower growth rate caused by its more complex composition and higher structural symmetry. The competitive growth between these two phases leads to a good possibility to produce nanostructured materials with interesting

properties in this alloy after annealing. This finding directly confirms the intrinsic correlation between the atomic clusters existing in MGs and the primary phases developed during crystallization of MGs and provides a new scenario for understanding the crystallization behavior of MGs.

ACKNOWLEDGMENTS

The work was supported by the National Natural Science Foundation of China (Grant No. 50901006), the Research Fund for the Doctoral Program of Higher Education of China (Grant No. 20090006120025), and the Program of Introducing Talents of Discipline to Universities (Grant No. B07003). X.J.L. is also supported by the Postdoctoral Fellowship at Hong Kong Polytechnic University. C.T.L. is supported by the internal funding from Hong Kong Polytechnic University.

- ¹W. Klement, R. H. Willens, and P. O. L. Duwez, *Nature (London)* **187**, 869 (1960).
- ²D. B. Miracle, *Nature Mater.* **3**, 697 (2004).
- ³H. W. Sheng, W. K. Luo, F. M. Alamgir, J. M. Bai, and E. Ma, *Nature (London)* **439**, 419 (2006).
- ⁴X. J. Liu, G. L. Chen, X. Hui, T. Liu, and Z. P. Lu, *Appl. Phys. Lett.* **93**, 011911 (2008).
- ⁵D. Ma, A. D. Stoica, and X. L. Wang, *Nature Mater.* **8**, 30 (2009).
- ⁶H. L. Peng, M. Z. Li, W. H. Wang, C. Z. Wang, and K. M. Ho, *Appl. Phys. Lett.* **96**, 021901 (2010).
- ⁷S. Mechler, G. Schumacher, I. Zizak, M. P. Macht, and N. Wanderka, *Appl. Phys. Lett.* **91**, 021907 (2007).
- ⁸L. Q. Xing, T. C. Hufnagel, J. Eckert, W. Loser, and L. Schultz, *Appl. Phys. Lett.* **77**, 1970 (2000).
- ⁹J. Sietsma and B. J. Thijsse, *J. Non-Cryst. Solids* **135**, 146 (1991).
- ¹⁰N. Mattern, U. Kühn, H. Hermann, H. Ehrenberg, J. Neufelnd, and J. Eckert, *Acta Mater.* **50**, 305 (2002).
- ¹¹X. J. Liu, X. D. Hui, H. Y. Hou, T. Liu, and G. L. Chen, *Phys. Lett. A* **372**, 3313 (2008).
- ¹²L. Huang, C. Z. Wang, S. G. Hao, M. J. Kramer, and K. M. Ho, *Phys. Rev. B* **81**, 094118 (2010).
- ¹³D. Ma, A. D. Stoica, X. L. Wang, Z. P. Lu, M. Xu, and M. Kramer, *Phys. Rev. B* **80**, 014202 (2009).
- ¹⁴Z. D. Sha, B. Xu, L. Shen, A. H. Zhang, Y. P. Feng, and Y. Li, *J. Appl. Phys.* **107**, 063508 (2010).
- ¹⁵D. R. Nelson, *Solid State Phys.*, Adv. Res. Appl. **42**, 1 (1989).
- ¹⁶T. Schenk, D. Holland-Moritz, V. Simonet, R. Bellissent, and D. M. Herlach, *Phys. Rev. Lett.* **89**, 075507 (2002).
- ¹⁷Y. Q. Cheng, E. Ma, and H. W. Sheng, *Phys. Rev. Lett.* **102**, 245501 (2009).
- ¹⁸K. F. Kelton, G. W. Lee, A. K. Gangopadhyay, R. W. Hyers, T. J. Rathz, J. R. Rogers, M. B. Robinson, and D. S. Robinson, *Phys. Rev. Lett.* **90**, 195504 (2003).
- ¹⁹F. C. Frank, *Proc. R. Soc. London, Ser. A* **215**, 43 (1952).
- ²⁰J. Eckert, N. Mattern, M. Zinkevitch, and M. Seidel, *Mater. Trans., JIM* **39**, 623 (1998).
- ²¹U. Köster, J. Meinhardt, S. Roos, and H. Liebertz, *Appl. Phys. Lett.* **69**, 179 (1996).
- ²²M. W. Chen, T. Zhang, A. Inoue, A. Sakai, and T. Sakurai, *Appl. Phys. Lett.* **75**, 1697 (1999).
- ²³G. L. Chen, X. J. Liu, X. D. Hui, H. Y. Hou, K. F. Yao, C. T. Liu, and J. Wadsworth, *Appl. Phys. Lett.* **88**, 203115 (2006).
- ²⁴X. J. Liu, G. L. Chen, X. D. Hui, H. Y. Hou, K. F. Yao, and C. T. Liu, *J. Appl. Phys.* **102**, 063515 (2007).
- ²⁵X. J. Liu, G. L. Chen, H. Y. Hou, X. Hui, K. F. Yao, Z. P. Lu, and C. T. Liu, *Acta Mater.* **56**, 2760 (2008).
- ²⁶T. H. Kim, A. K. Gangopadhyay, L. Q. Xing, G. W. Lee, Y. T. Shen, K. F. Kelton, A. I. Goldman, R. W. Hyers, and J. R. Rogers, *Appl. Phys. Lett.* **87**, 251924 (2005).
- ²⁷K. F. Kelton, W. J. Kim, and R. M. Stroud, *Appl. Phys. Lett.* **70**, 3230 (1997).

- ²⁸X. Qiu, J. W. Thompson, and S. J. L. Billinge, *J. Appl. Crystallogr.* **37**, 678 (2004).
- ²⁹T. E. Faber and J. M. Ziman, *Philos. Mag.* **11**, 153 (1965).
- ³⁰Z. Zhu, W. Zhang, G. Xie, and A. Inoue, *Appl. Phys. Lett.* **97**, 031919 (2010).
- ³¹S. Sachdev and D. R. Nelson, *Phys. Rev. Lett.* **53**, 1947 (1984).
- ³²X. J. Liu, X. D. Hui, J. T. Jiao, and G. L. Chen, *Trans. Nonferrous Met. Soc. China* **14**, 858 (2004).
- ³³H. Assadi and J. Schroers, *Acta Mater.* **50**, 89 (2002).
- ³⁴J. Saida, M. Sherif El-Eskandarany, and A. Inoue, *Scr. Mater.* **48**, 1397 (2003).
- ³⁵C. Li and A. Inoue, *Phys. Rev. B* **63**, 172201 (2001).
- ³⁶X. J. Liu, X. D. Hui, G. L. Chen, and M. H. Sun, *Intermetallics* **16**, 10 (2008).